nature structural & molecular biology

A distinct mechanism for the ABC transporter BtuCD–BtuF revealed by the dynamics of complex formation

Oded Lewinson[1], Allen T Lee[1,2], Kaspar P Locher[3] & Douglas C Rees[1,2]

ATP-binding cassette (ABC) transporters are integral membrane proteins that translocate a diverse array of substrates across cell membranes. We present here the dynamics of complex formation of three structurally characterized ABC transporters—the BtuCD vitamin B_{12} importer and MetNI D/L-methionine importer from *Escherichia coli* and the Hi1470/1 metal-chelate importer from *Haemophilus influenzae*—in complex with their cognate binding proteins. Similarly to other ABC importers, MetNI interacts with its binding protein with low affinity (K_d ~10^{-4} M). In contrast, BtuCD–BtuF and Hi1470/1–Hi1472 form stable, high-affinity complexes (K_d ~10^{-13} and 10^{-9} M, respectively). In BtuCD–BtuF, vitamin B_{12} accelerates the complex dissociation rate ~10^7-fold, with ATP having an additional destabilizing effect. The findings presented here highlight substantial mechanistic differences between BtuCD–BtuF, and likely Hi1470/1–Hi1472, and the better-characterized maltose and related ABC transport systems, indicating that there is considerable mechanistic diversity within this large protein super-family.

ATP-binding cassette (ABC) transporters comprise a ubiquitous superfamily of proteins present in all kingdoms of life[1,2]. These transporters couple the energy of ATP hydrolysis to the translocation of a diverse array of substrates across biological membranes. A large body of experimental evidence supports a 'two-state, alternating-access' mechanistic model for ABC exporters and importers[3–6]. In this model, ATP binding, hydrolysis and product release drive the conformational changes of the transporter between two major states: an outward-facing conformation, in which the substrate binding site is exposed to the extracellular side of the membrane, and an inward-facing conformation, in which the binding site is exposed to the cytoplasm. In concert with changes in the affinity of the binding site toward the substrate, these conformational changes ensure net substrate uptake by an importer or net expulsion by an exporter.

ABC transporters that import essential nutrients into cells depend on a high-affinity binding protein for their function[7–9]. The binding protein acts as a substrate chaperone that shuttles back and forth from the periplasm to the transporter to deliver substrate molecules. The integration of the binding protein into the above-mentioned two-state model is such that a substrate-loaded binding protein associates with the ATP-bound transporter, thus facilitating closure of the nucleotide-binding domains and stabilizing the outward-facing conformation[10,11]. ATP hydrolysis and subsequent phosphate release drive a conformational change to the inward-facing conformation, followed by substrate release and dissociation of the transporter–binding protein complex. This scheme of events is perhaps best exemplified by the maltose transporter, as has been comprehensively shown[4].

In *Escherichia coli* and other Gram-negative bacteria, vitamin B_{12} transport across the outer membrane is mediated by the collaborative action of BtuB, a high-affinity, β-barrel–type outer membrane transporter, and TonB, a periplasmic protein[12,13]. Once vitamin B_{12} accumulates in the periplasm, its passage through the inner membrane depends on the action of BtuCD, the *E. coli* vitamin B_{12} ABC transporter, and BtuF, its high-affinity cognate substrate-binding protein[14]. Several observations in the *E. coli* vitamin B_{12} ABC transport system suggest that BtuCD–BtuF operates by a distinct mechanism relative to that established for the maltose transporter and related ABC transporters. The vitamin B_{12} binding protein BtuF has been shown to form an extremely stable complex with BtuCD[15,16]. Such an essentially irreversible interaction is inconsistent with a mechanism in which the binding protein associates and dissociates from the transporter during each transport cycle. In addition, upon ATP binding, an electronic paramagnetic resonance spin label attached to the cytoplasmic gate shows increased mobility[17]. Although this observation does not provide direct proof, it is compatible with opening of this gate to the cytoplasm upon ATP binding.

To better characterize the mechanism of vitamin B_{12} transport, we have studied in detail the dynamic nature of association and dissociation between BtuCD (the transporter) and BtuF (the binding protein) using surface plasmon resonance (also termed BiaCore (GE Healthcare)). We have complemented these studies with several other experimental approaches, and in the present report, we delineate the kinetic and energetic relationships characterizing the interactions between the transporter, binding protein and substrate. The results indicate that BtuCD operates by a mechanism distinct from that proposed for the maltose transporter and related ABC transporters. We propose that ABC importers can be divided into groups that differ not only phylogenetically[4,18] and structurally[5,19], but also mechanistically. We support this hypothesis with the preliminary characterization of two additional structurally characterized

[1]Division of Chemistry and Chemical Engineering and [2]Howard Hughes Medical Institute, California Institute of Technology, Pasadena, California, USA. [3]Institute of Molecular Biology and Biophysics, ETH Zurich, Zurich, Switzerland. Correspondence should be addressed to D.C.R. (dcrees@caltech.edu).

Received 9 June 2009; accepted 25 November 2009; published online 21 February 2010; doi:10.1038/nsmb.1770

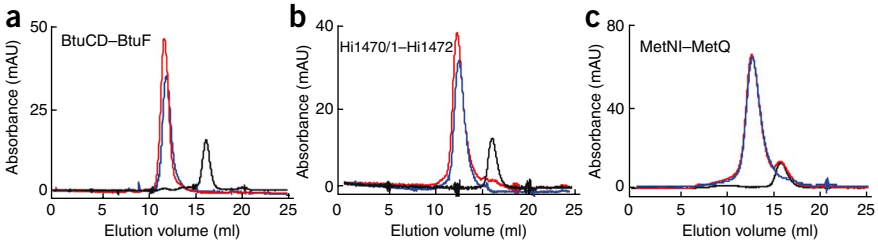

Figure 1 Complex formation between ABC transporters and their respective binding proteins. (**a**–**c**) BtuCD–BtuF (**a**), Hi1470/1-2 (**b**) and MetNI–MetQ (**c**). Size-exclusion chromatography of ABC transporters injected individually (blue traces) or after incubation with their binding proteins (red traces). Also shown are results of equimolar injections of the binding proteins (black traces). Stable complex formation is characterized by a shift in the location, and a slight increase in area, of the transporter peak and by the disappearance of the binding protein peak. In **a** and **b**, injections were at a 1:1 molar ratio (transporter:binding protein); in **c**, a 3:1 molar ratio. mAU, milli absorbance units.

ABC import systems: the D/L-methionine transporter MetNI–MetQ and the metal-chelate transporter Hi1470/1–Hi1472.

RESULTS

Association between importers and their binding proteins

Models of binding protein–dependent ABC transporters depict a short-lived association between the transporter and its soluble binding protein, in which the binding protein shuttles between the periplasm and the transporter to deliver substrate molecules. However, the association between the vitamin B_{12} transporter BtuCD and its binding protein, BtuF, does not fit this model. As shown by gel-filtration experiments, when BtuF is prepared in the absence of substrate and then mixed with BtuCD at a 1:1 molar ratio, virtually all BtuF is in complex with the transporter, and none can be detected in free form (**Fig. 1a**). This complex can then be isolated and is extremely stable[16]. Similar results were obtained with the *H. influenzae* putative metal-chelate ABC import system, Hi1470/1–Hi1472. Prior to injection, incubation of this transporter with its binding protein at a 1:1 molar ratio results in a shift in the location, and an increase in area, of the transporter peak, accompanied by an almost complete disappearance of the binding-protein peak (**Fig. 1b**). In contrast to these two observations, yet similar to what has been reported for the maltose and histidine uptake systems, no complex formation was observed in the methionine uptake system, even when the transporter (MetNI) was present at a 5-, 10- or 20-fold molar excess of the binding protein (MetQ; **Fig. 1c** and data not shown).

We used surface plasmon resonance to further characterize the interactions between ABC transporters and their binding proteins. We immobilized BtuCD, Hi1470/1 and MetNI via histidine (His) tags on a BiaCore chip. Following immobilization, we injected non–His-tagged binding proteins (BtuF, Hi1472 or MetQ, respectively) onto the flow cells. **Figure 2a–c** shows the specificity of the BiaCore system: the transporters interacted only with their cognate binding proteins, and not with binding proteins from different systems. When we flowed 20 nM BtuF over a flow cell onto which we had immobilized BtuCD, we obtained a robust response representing complex formation (**Fig. 2a**). Once the injection was terminated (and washing of the chip with buffer began), the complex was stable and did not dissociate. Similarly, upon injection of 20 nM Hi1472 over immobilized Hi1470/1, the two rapidly associate, and we observed complete dissociation only after 30–40 min (**Fig. 2b**). A much higher concentration (15 μM) was necessary to elicit a proportional response when injecting MetQ over immobilized MetNI. We also observed complex formation in this system (**Fig. 2c**); however, in contrast to the previous two transport systems, upon termination of MetQ injection (and commencement of chip washing with buffer), the MetNI–MetQ complex quickly dissociated. The different kinetic behavior of the three import systems is further illustrated in **Figure 2d–f**, depicting a series of concentrations of the binding proteins injected over a constant concentration of the transporters.

The association and dissociation curves of all three systems showed clear biphasic characteristics and were better described by applying fitting models that take into account a possible conformational change upon association (see Online Methods). The initial association event (k_{a1} values in **Table 1**) of the three import systems was characterized by moderate to fast rates (~10^3–10^5 M^{-1} s^{-1}), with Hi1470/1–Hi1472 being the fastest and MetNI–MetQ the slowest. As can be appreciated by a visual comparison of **Figure 2d–f**, greater variance was observed for the dissociation rates. Whereas the k_{d1} for BtuCD–BtuF is almost negligible at ~10^{-8} s^{-1} (i.e. ~2×10^{-3} d^{-1}), the corresponding value for MetNI–MetQ, ~0.2 s^{-1} (**Table 1**), is compatible with measured transport rates of ABC transporters[20–22]. Derivation of the equilibrium dissociation constants (K_d) from the rate constants given in **Table 1** yield high (10^{-13} M), medium (~10^{-9} M) and low (10^{-4} M) affinities

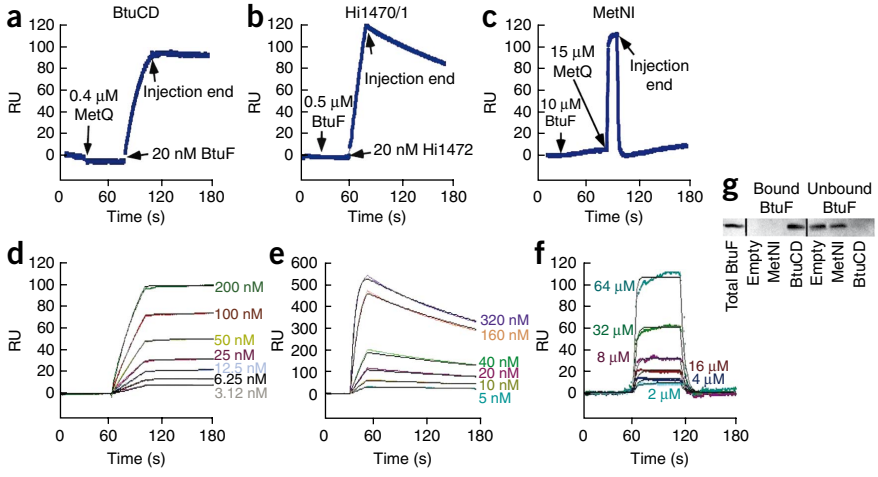

Figure 2 Dynamics of complex formation. BtuCD–BtuF (**a**,**d**), Hi1470/1–Hi1472 (**b**,**e**) and MetNI–MetQ (**c**,**f**) import systems. The transporters (~30 ng) were immobilized onto a BiaCore chip and subjected to the following: shown in **a**–**c** are injections of BtuF, Hi1472 or MetQ as indicated by the arrows. Shown in **d**–**f** are injections of the indicated concentrations of BtuF, Hi1472 or MetQ, respectively. Black traces in **d**–**f** are the fits to the experimental data curves. Standard errors for these fits are given in **Table 1**. RU, resonance units. (**g**) Association of BtuF and BtuCD in proteoliposomes. 20 nM Flag-tagged BtuF was added to empty liposomes or proteoliposomes reconstituted with either MetNI or BtuCD as indicated. The liposome-bound and unbound fractions of BtuF were separated and visualized by immunoblot detection.

Table 1 Kinetic rate constants determined in BiaCore experiments for the BtuCD–BtuF, Hi1470/1–Hi1472 and MetNI–MetQ import systems

Transport system	Additives	k_{a1} ($M^{-1}s^{-1}$)	k_{d1} (s^{-1})	k_{a2} (s^{-1})	k_{d2} (s^{-1})	K_d (M)
Vitamin B_{12}	None	$(4.54 \pm 0.05) \times 10^4$	$(1.12 \pm 0.28) \times 10^{-8}$	$(1.12 \pm 0.06) \times 10^{-3}$	$(9.95 \pm 0.18) \times 10^{-4}$	1.16×10^{-13}
	Vitamin B_{12}	$(3.85 \pm 0.15) \times 10^5$	1.51 ± 0.05	$(2.37 \pm 0.02) \times 10^{-3}$	$(1.28 \pm 0.37) \times 10^{-5}$	2.11×10^{-8}
	ATP/EDTA	$(9.58 \pm 0.07) \times 10^3$	$(1.36 \pm 0.09) \times 10^{-6}$	$(1.67 \pm 0.39) \times 10^{-3}$	$(9.79 \pm 0.38) \times 10^{-4}$	6.23×10^{-11}
	ATP/EDTA + vitamin B_{12}			No association detected		
	ATP, Mg^{2+}, vanadate	$(5.51 \pm 0.22) \times 10^4$	$(2.03 \pm 0.19) \times 10^{-6}$	$(1.01 \pm 0.09) \times 10^{-3}$	$(9.97 \pm 0.84) \times 10^{-5}$	1.76×10^{-11}
	ATP, Mg^{2+}, vanadate + vitamin B_{12}			No association detected		
	ADP, Mg^{2+}	$(4.82 \pm 0.06) \times 10^5$	$(3.01 \pm 0.01) \times 10^{-4}$	$(2.06 \pm 0.05) \times 10^{-2}$	$(5.2 \pm 0.21) \times 10^{-4}$	4.95×10^{-13}
	ADP, Mg^{2+} + vitamin B_{12}	$(2.10 \pm 0.04) \times 10^4$	0.99 ± 0.01	$(2.02 \pm 0.03) \times 10^{-2}$	$(1.59 \pm 0.52) \times 10^{-5}$	3.34×10^{-8}
	ATP, Mg^{2+} + vitamin B_{12}	$(3.73 \pm 0.00) \times 10^4$	0.77 ± 0.01	$(5.14 \pm 0.01) \times 10^{-2}$	$(9.02 \pm 7.3) \times 10^{-6}$	3.6×10^{-9}
Putative metal chelate	None	$(8.83 \pm 0.07) \times 10^5$	$(1.01 \pm 0.06) \times 10^{-2}$	$(4.55 \pm 0.41) \times 10^{-2}$	$(4.01 \pm 0.08) \times 10^{-2}$	5.72×10^{-9}
D/L-methionine	None	$(3.08 \pm 0.20) \times 10^3$	0.23 ± 0.04	$(9.55 \pm 0.40) \times 10^{-7}$	$(9.00 \pm 3.00) \times 10^{-2}$	7.40×10^{-5}

k_{a1} and k_{d1}, forward and reverse rate constants of the initial association leading to complex formation; k_{a2} and k_{d2}, forward and reverse rate constants of the conformational change following complex formation; K_d, dissociation constant calculated from derived rate constants (see Online Methods).

for BtuCD–BtuF, Hi1470/1–Hi1472 and MetNI–MetQ, respectively. The ~100 μM K_d (7.4×10^{-5} M) of the MetNI–MetQ interaction is in agreement with its anticipated low affinity, as suggested by the gel filtration results (**Fig. 1c**). Similarly low affinities have been reported for the maltose, histidine and oligopeptide systems[9,23,24]. Whereas the k_{a1} for the three studied systems differ by 2 orders of magnitude, the k_{d1} and equilibrium constants vary by up to 8 orders of magnitude (**Table 1**), indicating that the dominant contributions to changes in binding affinities reflect variations in the dissociation rate constants.

To study whether a high-affinity BtuCD–BtuF complex also forms in the membrane milieu, we reconstituted BtuCD into liposomes. We then compared the interaction of BtuCD liposomes with BtuF to the interactions of BtuF with either empty liposomes or liposomes reconstituted with MetNI. We added BtuF (20 nM) to liposomes or proteoliposomes containing equal amounts of either BtuCD or MetNI. Following a 10-min incubation, we pelleted the liposomes by ultracentrifugation. Most, if not all, of the added BtuF was bound to the BtuCD liposomes, whereas none associated with either the MetNI liposomes or the empty liposomes (**Fig. 2g**). In contrast, we detected no unbound BtuF in the soluble fraction of the BtuCD liposomes, and all of BtuF was found in the soluble fractions of the MetNI liposomes and the empty liposomes. The seemingly complete binding of BtuF by BtuCD liposomes indicates that the K_d of the interaction is lower than 20 nM. Lower BtuF concentrations could not be tested because 20 nM is the detection limit of this SDS-PAGE–based assay (see Online Methods).

Vitamin B_{12} binding and release

The stability of the transporter–binding protein complex, characteristic of the vitamin B_{12} and Hi1470/1–Hi1472 uptake systems, prompted speculations that perhaps this complex is responsible for substrate binding[20]. Vitamin B_{12} forms a pinkish aqueous solution with an absorbance maximum at 360 nm, which enables detection of its association with proteins. We purified BtuCD, BtuF and the BtuCD–BtuF complex to homogeneity and analyzed them by size-exclusion chromatography before (**Fig. 3a**) or after (**Fig. 3b**) incubation with vitamin B_{12}. When BtuCD was incubated with 50 μM vitamin B_{12}, we observed no 360-nm absorbance in the fractions corresponding to the 280-nm elution peak of the transporter. Additions of ATP and Mg^{2+}, ADP and Mg^{2+}, AMP-PNP and Mg^{2+}, AMP-PCP and Mg^{2+} or ATP and EDTA (see Online Methods for details) yielded identical 360-nm elution profiles, suggesting that, regardless of its nucleotide state, BtuCD does not bind vitamin B_{12} with high affinity at the tested concentration range (10–100 μM). Much like the free transporter, the BtuCD–BtuF complex did not bind vitamin B_{12} (**Fig. 3b**), irrespective of the nucleotide state of the transport complex. In contrast to BtuCD or the BtuCD–BtuF complex, when we prepared the periplasmic binding protein BtuF in the absence of vitamin B_{12} and then incubated the BtuF in its presence, the two associated tightly, as indicated by the 360-nm peak eluting at ~17 ml and by the decrease in the amount of free vitamin B_{12} eluting at ~20.5 ml. These results are in agreement with the reported high affinity (~15 nM) of BtuF to B_{12} (ref. 14). Taken together, these results suggest that only free, uncomplexed BtuF binds substrate with high affinity, whereas the free transporter, or the transport complex, lacks this ability regardless of its nucleotide state.

A similar approach was employed to investigate substrate release in the BtuCD–BtuF transport system. In these experiments, we prepared the binding protein (BtuF) in the presence of a saturating concentration (10 μM) of vitamin B_{12}. When such a preparation was subjected to gel-filtration chromatography, two clear peaks can be distinguished at 360 nm, one eluting at ~17 ml and the other eluting at ~20.5 ml (**Fig. 4a**). These two peaks correspond to BtuF-bound vitamin B_{12} and free vitamin B_{12}, respectively. When the same preparation was subjected to a 10-fold or a 100-fold wash with buffer devoid of vitamin B_{12} (see Online Methods for details), the peak for free vitamin B_{12} diminished and all but disappeared, whereas the peak corresponding to the BtuF-bound vitamin B_{12} remained almost constant (**Fig. 4a**). This observation suggests that, under these conditions, vitamin B_{12} is not efficiently released from BtuF. When we mixed an identical preparation of vitamin B_{12}–loaded BtuF (washed 100-fold from any free vitamin B_{12}) with BtuCD at a molar ratio of 1:2 (BtuCD:BtuF), roughly half

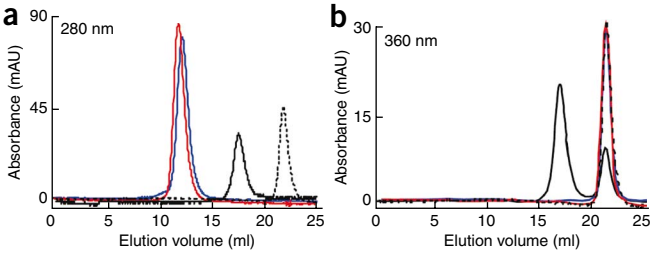

Figure 3 Substrate binding by components of the vitamin B_{12} transport system. (**a**,**b**) BtuCD (blue), BtuF (solid black) and the BtuCD–BtuF complex (red) were purified and subjected to size-exclusion chromatography before (**a**) or after (**b**) incubation with 50 μM vitamin B_{12} (dashed black). In **a** and **b**, absorbance was recorded at 280 nm and 360 nm, respectively. mAU, milli absorbance units.

of the 360-nm signal previously associated with BtuF appears as free vitamin B_{12} (**Fig. 4b**, blue trace). When vitamin B_{12}–loaded BtuF was mixed with BtuCD at a 1:1 molar ratio, almost all of the vitamin B_{12} appeared in free form. Addition of BtuCD in excess of BtuF (2:1 molar ratio) resulted in complete release of vitamin B_{12} from BtuF (**Fig. 4b**, dashed cyan trace). The small 360-nm peak that gradually appeared at ~14 ml reflects the small absorbance that BtuCD and the BtuCD–BtuF complex have at this wavelength. Vitamin B_{12} did not associate with either BtuCD or the BtuCD–BtuF complex, suggesting that, upon binding of BtuF to BtuCD, vitamin B_{12} is released from BtuF and is only transiently associated with the complex.

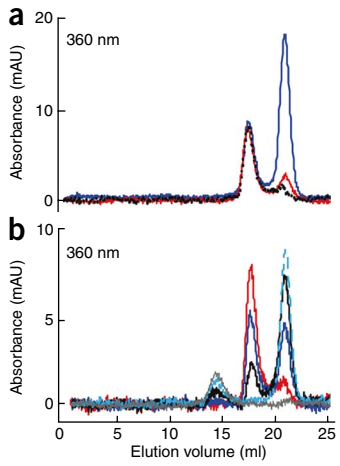

Figure 4 Substrate release from the vitamin B_{12} transport system. (**a**) BtuF was prepared in the presence of 10 μM vitamin B_{12} and subjected to separation by size-exclusion chromatography (blue). The same preparation was washed in a 10-fold (red) or 100-fold (dashed black) excess of buffer devoid of vitamin B_{12}. Absorbance was recorded at 360 nm. (**b**) An identical preparation of BtuF (washed 100-fold) was subjected to separation by size-exclusion chromatography before (red) or after incubation with BtuCD at 1:2 (blue), 1:1 (black) or 2:1 (dashed cyan) BtuCD:BtuF molar ratio. Also shown (in gray) is an injection of BtuCD at the highest concentration used. Absorbance was recorded at 360 nm. mAU, milli absorbance units.

Substrate effects on the association between BtuCD and BtuF

The effect of substrate on complex formation was investigated through BiaCore experiments in which BtuF was injected in the presence of increasing concentrations of vitamin B_{12} (**Fig. 5a**). Notably, the stability of the BtuCD–BtuF complex decreased in the presence of vitamin B_{12}. So pronounced was this effect that, in the presence of vitamin B_{12} concentrations >50 μM, the equilibrium affinity decreases by ~5 orders of magnitude (**Table 1**). The greatest effect of increasing the vitamin B_{12} concentrations occurred between 0.48 μM and 2.4 μM (**Fig. 5a**); this is most probably a result of the degree of occupancy of BtuF (1 μM was used in this experiment) by vitamin B_{12} rather than of the binding affinity of BtuF toward vitamin B_{12}.

We used two additional, independent experimental methods to validate this observation. In the first set of experiments, we used size-exclusion chromatography to qualitatively evaluate the effect of substrate on complex formation. When BtuF was prepared in the absence of substrate and was then incubated with a twofold molar excess of BtuCD, we did not observe a peak representing free BtuF, and practically all of the binding protein was associated with the transporter (**Fig. 5b**). When we added 100 μM vitamin B_{12} to BtuF before incubating it with BtuCD, all the BtuF appeared as a free, uncomplexed form (compare ~17-ml peak of red and black traces in **Fig. 5b**). We obtained similar results from pulldown experiments in which either His-tagged BtuCD or His-tagged BtuF were immobilized on nickel–nitrilotriacetic acid (Ni-NTA) beads and incubated with a Flag-tagged partner (see Online Methods for details). In these experiments, the amount of retained Flag-tagged protein was inversely related to the concentration of vitamin B_{12} (**Fig. 5c**). As observed in the BiaCore system (**Fig. 5a**), the greatest effect of the increasing vitamin B_{12} concentrations was between 233 nM and 2.85 μM, reflecting the BtuF concentration (~2 μM) used in this experiment.

We also studied substrate effects in a liposome-reconstituted system. In these experiments, 35 nM BtuF were added to BtuCD liposomes in the presence or absence of various concentrations of vitamin B_{12}. Similar to what has been observed in the solution experiments (Biacore, gel filtration, pulldowns), the affinity between BtuCD and BtuF decreased with increasing substrate concentrations (**Fig. 5d**).

To further characterize the observed substrate effects, rate constants of complex association and dissociation were determined in the presence of saturating vitamin B_{12} concentrations. Relative to the values determined in the absence of substrate, addition of substrate resulted in a modest (10- to 20-fold) stimulation of k_{a1} (**Fig. 6a** and **Table 1**). However, most remarkable was the substrate-induced stimulation of complex dissociation: in the presence of vitamin B_{12}, the k_{d1} of the initial interaction was accelerated by ~8 orders of magnitude, from 1.12×10^{-8} s^{-1} to 1.55 s^{-1} (**Fig. 2d**, **Fig. 6a** and **Table 1**). The equilibrium dissociation constant ($K_d = 2.11 \times 10^{-8}$ M) calculated between the binding protein and transporter in the presence of vitamin B_{12} is consistent with the substrate-induced decrease in equilibrium affinity described above (**Fig. 5**).

Effects of nucleotide on BtuCD–BtuF association and dissociation

We measured the effects of nucleotide binding and hydrolysis on the interactions between BtuCD and BtuF at several conditions that

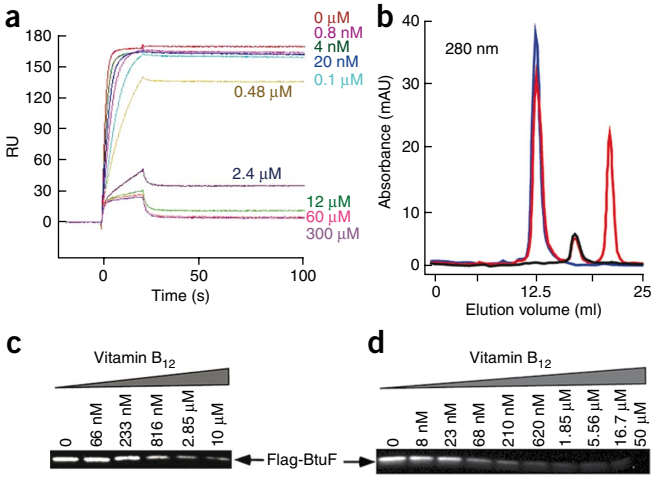

Figure 5 Substrate effects on complex formation in the vitamin B_{12} transport system. (**a**) BiaCore experiments: His-tagged BtuCD (~30 ng) was immobilized onto a Ni-NTA chip. At 0 s, 1 μM BtuF was injected in the presence of 0–300 μM vitamin B_{12} as indicated. RU, resonance units. (**b**) Size- exclusion chromatography. The following preparations were analyzed by gel-filtration chromatography: BtuF prepared in the absence of vitamin B_{12} and mixed with BtuCD (blue) and BtuF prepared in the presence of 100 μM vitamin B_{12} and then mixed with BtuCD (red). An identical amount of BtuF was injected by itself (black). All traces were recorded at 280 nm. mAU, milli absorbance units. (**c**) Pulldown experiments. His-tagged BtuCD was immobilized onto Ni-NTA resin and incubated with 2 μM Flag-BtuF in the absence or presence of the indicated vitamin B_{12} concentrations. Unbound protein was removed and the amount of retained Flag-BtuF was visualized by immunodetection using an anti-Flag antibody. (**d**) Complex formation in proteoliposomes. We added 35 nM Flag-tagged BtuF to BtuCD proteoliposomes, in the absence or presence of the indicated vitamin B_{12} concentrations. Bound and unbound BtuF were separated as detailed in Online Methods. The amount of Flag-BtuF was visualized by immunodetection using an anti-Flag antibody.

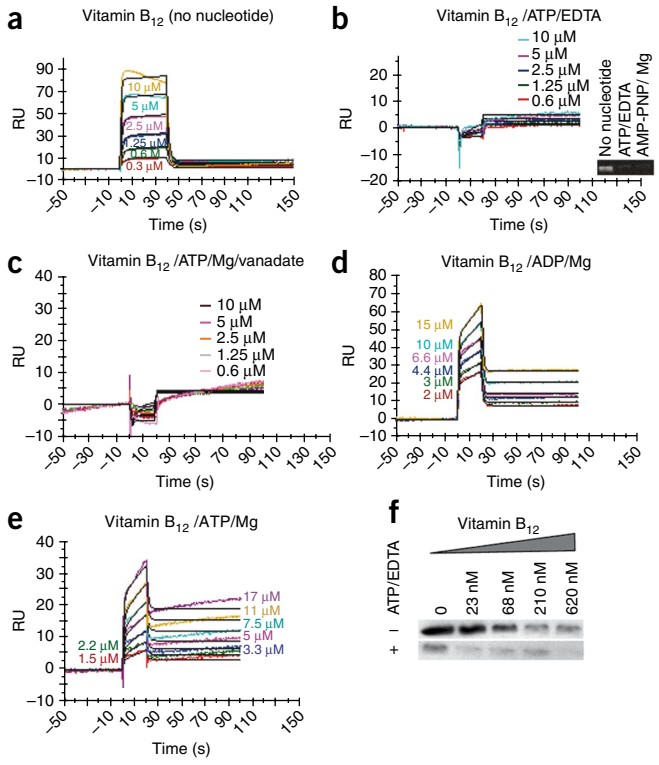

Figure 6 Effects of nucleotide binding and hydrolysis on complex formation in the vitamin B_{12} transport system. (**a**–**e**) The indicated BtuF concentrations were injected in the presence of 200 μM vitamin B_{12} and no further addition (**a**), 1 mM ATP, 50 μM EDTA (**b**), 1 mM ATP, 2 mM $MgSO_4$, 1 mM orthovanadate (**c**), 1 mM ADP, 2 mM $MgSO_4$ (**d**) and 1 mM ATP, 2 mM $MgSO_4$ (**e**). Black traces are the fits to the experimental data curves. Standard errors for these fits are given in **Table 1**. Inset in **b** shows pulldown experiment of Ni-NTA–immobilized His-tagged BtuCD incubated with Flag-tagged BtuF in the presence of 25 μM vitamin B_{12}, in the absence of nucleotide or in the presence of 1 mM ATP, 50 μM EDTA or 1 mM AMP-PNP, 2 mM $MgSO_4$ as indicated. The amount of retained Flag-BtuF was visualized by immunodetection using an anti-Flag antibody. RU, resonance units. (**f**) Interaction in the membrane. BtuCD liposomes were prepared in the absence (top) or presence (bottom) of 1 mM ATP, 50 μM EDTA. We added 35 nM Flag-tagged BtuF to the liposomes in the presence of the indicated vitamin B_{12} concentrations. Bound and unbound BtuF were separated as detailed in Online Methods. The amount of Flag-BtuF was visualized by immunodetection using an anti-Flag antibody.

presumably mimic the sequential steps of ATP hydrolysis (**Fig. 6**). We verified the binding of nucleotides by BtuCD and BtuCD–BtuF by measuring the 260/280 nm absorbance ratios in the absence or presence of ATP, and by conducting ATP hydrolysis assays (see **Supplementary Methods** and **Supplementary Fig. 1**). Notably, in the presence of vitamin B_{12}, upon binding of ATP (or ATP analogs) no association between BtuF and BtuCD could be detected (compare **Fig. 6a**,**b**). We also observed the reduced affinity between the nucleotide-bound transporter and the substrate-loaded binding protein in pulldown experiments. Using this approach, we readily observed complex formation in the nucleotide-free state, yet it was undetectable in the nucleotide-bound state (**Fig. 6b**, inset). Notably, the lack of interaction between BtuCD and BtuF was not due to any destabilizing effects of nucleotide binding on BtuCD (**Supplementary Fig. 2**).

We also studied the combined effect of substrate and nucleotide binding in the liposome-reconstituted system. In these experiments, BtuCD-reconstituted liposomes were prepared in the presence or absence of 1 mM ATP, 50 μM EDTA. As shown (**Fig. 6f**), ATP binding by membrane-embedded BtuCD decreased its affinity to BtuF both in the absence or presence of substrate. Such was this effect that, in the presence of ATP, EDTA and saturating concentrations of vitamin B_{12}, no complex formation could be detected.

Concomitant additions of ATP, magnesium and vanadate have been used to trap ABC transporters[25,26] and BtuCD[20] (**Supplementary Fig. 1**) in a transition state analog of ATP hydrolysis. Similar to what has been observed in the nucleotide-bound state, in the presence of vitamin B_{12}, no complex formation could be detected with this transition-state mimic (**Fig. 6c**). Notably, in the maltose ABC import system, this state induces the highest affinity between the maltose transporter and the maltose binding protein[21,27]; it seems that the opposite is true for the vitamin B_{12} ABC transport system.

The posthydrolysis, ADP-bound state is shown in **Figure 6d**. In this state, complex formation and dissociation are once again readily detected with kinetic constants similar to that of the nucleotide-free state (**Table 1**).

Generation of hydrolytic conditions by addition of magnesium ATP (Mg-ATP) likely results in a mixed population of BtuCD molecules as they progress through the various conformations accompanying ATP binding and hydrolysis. This ensemble of conformations comprises four of the above-mentioned states (**Fig. 6a–d**). Thus, the kinetic parameters measured under hydrolyzing conditions are a weighted average, dictated by the proportion of the molecules residing at each state as well as the average dwell time in each state. A sensogram recording made in the presence of vitamin B_{12} and Mg-ATP (**Fig. 6e**) shows rate constants most similar to those determined in the absence of nucleotide or in the presence of Mg-ADP (**Table 1**). Considering the high levels of cellular ATP, this suggests that on average, ATP-hydrolyzing BtuCD molecules reside longer in the ADP-bound state than in the prehydrolysis (ATP-bound) or transition-state–like (Mg-ATP/vanadate) intermediates, where we observed no association.

DISCUSSION

In the present study, we report in detail the effects of substrate and nucleotide binding on the formation of the BtuCD–BtuF vitamin B_{12} transport complex. As discussed below, a synopsis of the current data suggest a distinct mechanism of transport in this system relative to the model developed for the more extensively characterized maltose ABC transporter.

In the absence of vitamin B_{12}, BtuF at concentrations above 10^{-11} M will be bound by BtuCD. Our previous[20] and current (**Supplementary Fig. 1**) results indicate that the BtuCD–BtuF complex binds and hydrolyzes ATP at least as efficiently as free BtuCD, both in proteoliposomes and in solution. We expect this substrate-free complex to shift through the energetic minima depicted in the bottom left corners of panels I–IV of the thermodynamic scheme shown in **Figure 7a**. The high intrinsic stability of the complex presents a considerable energetic hurdle for productive transport: the crystal structure of BtuCD–BtuF[16] indicates that once the complex has formed, vitamin B_{12} cannot access the binding site. This notion is supported here by the observation that the complex is unable to bind substrate (**Fig. 3**). Hence, the complex must dissociate for transport to occur (**Fig. 7b**, state I). Complex dissociation is facilitated by both substrate and ATP (**Figs. 5** and **6**). However, other factors may also affect the association of BtuCD and BtuF. For example, through its interaction with BtuF, TonB[28] may influence the formation of the BtuCD–BtuF complex. In addition, tight transcriptional and/or translational control (as observed in the vitamin B_{12} uptake system and related systems[29–31]) may prevent expression of BtuCD–BtuF in the absence of substrate. Clearly, further studies are required to resolve these complexities.

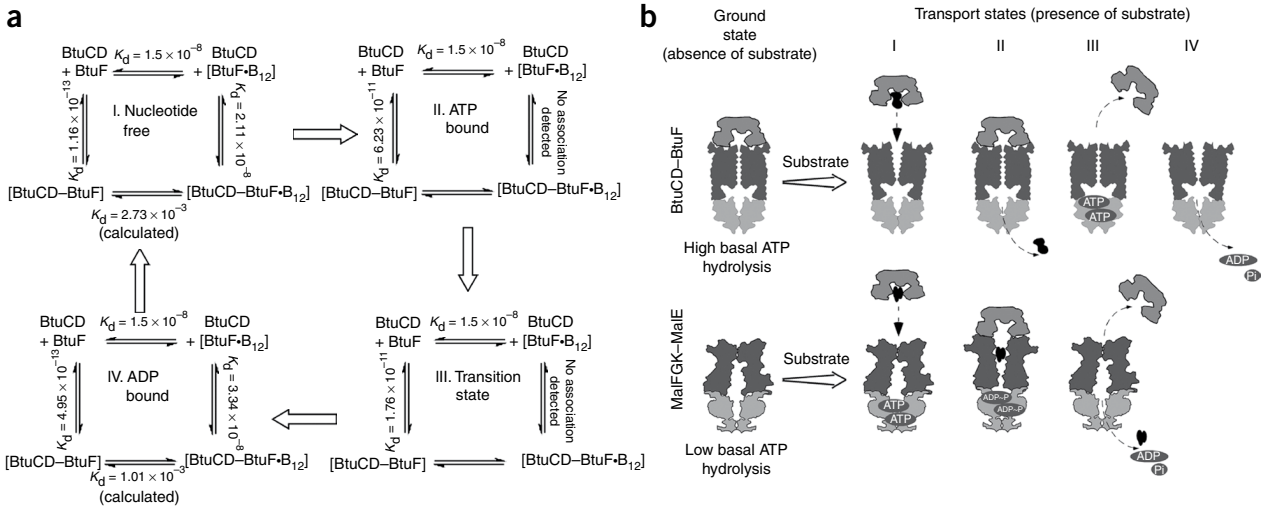

Figure 7 Thermodynamics of the BtuCD-F transport cycle and comparison to the maltose system. (**a**) Thermodynamic scheme summarizing the equilibrium constants determined for the vitamin B_{12} transport system. Each panel represents a different nucleotide state of BtuCD: the horizontal reactions describe vitamin B_{12} binding and release, whereas the vertical reactions are for the formation and dissociation of the BtuCD–BtuF complex. In each panel, the vertical left and right reactions are for BtuCD–BtuF complex formation in the absence and presence of vitamin B_{12}, respectively. Unless otherwise indicated, all values were experimentally determined. (**b**) Mechanistic differences between the maltose transporter and BtuCD–BtuF. The ground state of the vitamin B_{12} system is the stable BtuCD–BtuF complex, which has high levels of basal ATPase activity. In the maltose system, the corresponding state is that of the free transporter, with low levels of ATPase activity. In both systems, the transition to the transport states is driven by substrate. Vitamin B_{12} drives complex dissociation, whereas maltose, by stabilizing the closed conformation of MalE, contributes to complex stability. The MalFGK–MalE complex is stabilized by ATP binding (or transition state, panel II), whereas the BtuCD–BtuF complex is destabilized by ATP binding (panel III).

As vitamin B_{12} is transported into the periplasm by BtuB and TonB, it can only be efficiently bound by BtuF, which is the only component of the system with high substrate affinity[14] (**Fig. 3**). Neither BtuCD nor BtuCD–BtuF has high affinity for substrate, regardless of its nucleotide state; accordingly, thermodynamic considerations (**Fig. 7a**, horizontal bottom constants of panels I and IV) provide an estimate of 10^{-3} M for the affinity between BtuCD–BtuF and vitamin B_{12}.

Upon association of vitamin B_{12}–loaded BtuF and BtuCD, substrate is released from BtuF and is not retained by the complex (**Fig.4** and **Fig. 7b**, state II). These findings are in agreement with the absence of vitamin B_{12} from the published crystal structure of the BtuCD–BtuF complex (despite the fact that this complex was prepared by incubating vitamin B_{12}–loaded BtuF with BtuCD[16]). Clearly, our present work could not determine the directionality of substrate release as these experiments were conducted in solution (**Fig. 4**). It is possible that in our solution experiments, vitamin B_{12} is released at the *cis* side via an 'escape pathway' rather than being properly released at the *trans* side (productive transport). If indeed such an escape pathway occurs, this may explain the poor transport stoichiometry (~100 ATP per vitamin B_{12}) measured in reconstituted proteoliposomes[20].

The key findings of the present report contrast with the mechanistic model that has been established in detail for the maltose transporter (**Fig. 7b**) and, to varying degrees, for other ABC transporters[11,32]. In the histidine and maltose import systems, substrate-free or substrate-loaded binding proteins interact with similar equilibrium affinity (micromolar range) with the transporter[24,27]. In the oligopeptide import system (OppABCDF), the presence of substrate greatly increases the affinity between the membrane-embedded transporter and its receptor[9]. As reported here, a very different substrate effect is observed in the BtuCD–BtuF system, where vitamin B_{12} accelerates complex formation 10- to 20-fold and complex dissociation ~10^7-fold, resulting in a ~10^5 drop in equilibrium affinity (**Figs. 5**, **6** and **7**, **Table 1**). The effects of vitamin B_{12} on the kinetics of interaction between BtuCD and BtuF underline the importance of conducting pre-equilibrium measurements of ABC transport systems.

Another mechanistic aspect that seems to differ between ABC transporters is the effect of binding protein on the rate of ATP hydrolysis. In the maltose and histidine systems, marked increase in ATPase rates is induced only by association of substrate-loaded binding protein with the transporter. In contrast, very modest stimulation (less than twofold[20]; **Supplementary Fig. 1**) of ATP hydrolysis rate is observed upon formation of the BtuCD–BtuF complex, and this low-level stimulation is conferred by substrate-free and substrate-loaded binding protein alike. With the exception of the transported associated with antigen processing system[33,34], low levels of substrate-induced stimulation of ATPase rates also seem to be a feature of ABC exporters, especially multidrug transporters[35–37]. The differences in substrate-induced effects on the interaction between the binding protein and the transporter (and its outcome) is perhaps related to the extent of substrate-induced conformational changes of the binding proteins: the maltose and histidine binding proteins (of type I ABC importers) undergo appreciable structural rearrangements upon substrate binding[38]. In comparison, ShuT[39], PhuT[40], FhuD[41] and BtuF[15,42] (binding proteins of type II ABC importers) show modest conformational changes upon substrate binding.

BtuCD has the lowest affinity for BtuF in the ATP-bound or transition-state analog–bound forms (**Fig. 7a**, panels II and III; **Fig. 7b**, state III; **Fig. 6**; **Table 1**). In its nucleotide-free state, BtuCD has the highest affinity toward BtuF. Again, this is in direct contrast to the maltose system, for which it was clearly shown that the nucleotide-bound transporter, and the transition-state analog for ATP hydrolysis, have the highest affinity toward the maltose binding protein, whereas the nucleotide-free form has the lowest (**Fig. 7b**, state II of bottom panel)[21]. Similarly, following release of vitamin B_{12}, the now– substrate-free BtuCD–BtuF complex represents the most stable, lowest-energy state of the transport cycle (**Fig. 7a**, panel I, bottom left corner). In comparison, the MalFGK–MalE complex is the highest-energy intermediate of the reaction, and under normal turnover conditions it is undetectable. In this respect, the putative metal-chelate import system (Hi1470/1–Hi1472) resembles BtuCD–BtuF as it forms a quasistable complex in the absence of nucleotide (**Figs. 1b** and **2b**,**e**), whereas

the D/L-methionine import system (MetNI–MetQ) forms a low-affinity complex (**Fig. 2c**,**f**) much like MalFGK–MalE or HisPQM–HisJ[23,24].

Sequence-based phylogenetic segregation of ABC transporters divides them into distinct evolutionary branches[18]. According to this classification, BtuCD–BtuF and Hi1470/1–Hi1472 are similar to each other and are relatively distant from the maltose, molybdate, histidine and methionine import systems. In addition to sequence conservation, recent comparisons of the crystal structures of ABC transporters suggest that the phylogenetic groups may also share a common fold of their membrane-spanning domain[5,19]. Thus, the maltose, molybdate and methionine import systems share a core fold that is distinct from the fold shared by BtuCD–BtuF and Hi1470/1–Hi1472. In the present report, we add another dimension to this picture, suggesting that members of different subclasses of ABC transporters differ not only in sequence and structure but also in mechanism. Further investigations of the genetic, structural and functional heterogeneity of ABC transporters will clearly advance our understanding of these elaborate cellular machines.

METHODS

Methods and any associated references are available in the online version of the paper at http://www.nature.com/nsmb/.

Note: Supplementary information is available on the Nature Structural & Molecular Biology website.

ACKNOWLEDGMENTS

We thank H. Pinkett for insightful discussions and critical reading of the manuscript and J. Klein and J. Vielmetter for their help in the initial BiaCore experiments. The work was supported in part by US National Institutes of Health grant GM045162, by the Howard Hughes Medical Institute and by fellowships to O.L. from the Fulbright Foundation and the Jane Coffin Childs Memorial Fund for Medical Research.

AUTHOR CONTRIBUTIONS

A.T.L. and K.P.L. generated the original constructs used in this work; O.L. and D.C.R. designed the research; O.L. and A.T.L. performed the research; O.L., A.T.L., K.P.L. and D.C.R. analyzed the data; and O.L., K.P.L. and D.C.R. wrote the paper.

COMPETING INTERESTS STATEMENT

The authors declare no competing financial interests.

Published online at http://www.nature.com/nsmb/.
Reprints and permissions information is available online at http://npg.nature.com/reprintsandpermissions/.

1. Higgins, C.F. ABC transporters: from microorganisms to man. *Annu. Rev. Cell Biol.* **8**, 67–113 (1992).
2. Higgins, C.F. ABC transporters: physiology, structure and mechanism–an overview. *Res. Microbiol.* **152**, 205–210 (2001).
3. van der Does, C. & Tampe, R. How do ABC transporters drive transport? *Biol. Chem.* **385**, 927–933 (2004).
4. Davidson, A.L., Dassa, E., Orelle, C. & Chen, J. Structure, function, and evolution of bacterial ATP-binding cassette systems. *Microbiol. Mol. Biol. Rev.* **72**, 317–364 (2008).
5. Locher, K.P. Review. Structure and mechanism of ATP-binding cassette transporters. *Phil. Trans. R. Soc. Lond. B* **364**, 239–245 (2009).
6. Jones, P.M., O'Mara, M.L. & George, A.M. ABC transporters: a riddle wrapped in a mystery inside an enigma. *Trends Biochem. Sci.* **34**, 520–531 (2009).
7. Boos, W. & Lucht, J.M. Periplasmic binding protein-dependent ABC transporters. in *Escherichia coli and Salmonella typhimurium: Cellular and Molecular Biology* Vol. 1 (ed. Neidhardt, F.C.) 1175–1209 (American Society for Microbiology, Washington, DC, 1996).
8. Rohrbach, M.R., Braun, V. & Koster, W. Ferrichrome transport in *Escherichia coli K-12*: altered substrate specificity of mutated periplasmic FhuD and interaction of FhuD with the integral membrane protein FhuB. *J. Bacteriol.* **177**, 7186–7193 (1995).
9. Doeven, M.K., Abele, R., Tampe, R. & Poolman, B. The binding specificity of OppA determines the selectivity of the oligopeptide ATP-binding cassette transporter. *J. Biol. Chem.* **279**, 32301–32307 (2004).
10. Orelle, C., Ayvaz, T., Everly, R.M., Klug, C.S. & Davidson, A.L. Both maltose-binding protein and ATP are required for nucleotide-binding domain closure in the intact maltose ABC transporter. *Proc. Natl. Acad. Sci. USA* **105**, 12837–12842 (2008).
11. Oldham, M.L., Khare, D., Quiocho, F.A., Davidson, A.L. & Chen, J. Crystal structure of a catalytic intermediate of the maltose transporter. *Nature* **450**, 515–521 (2007).
12. Bassford, P.J. Jr., Bradbeer, C., Kadner, R.J. & Schnaitman, C.A. Transport of vitamin B_{12} in tonB mutants of *Escherichia coli*. *J. Bacteriol.* **128**, 242–247 (1976).
13. Bassford, P.J. Jr. & Kadner, R.J. Genetic analysis of components involved in vitamin B_{12} uptake in *Escherichia coli*. *J. Bacteriol.* **132**, 796–805 (1977).
14. Cadieux, N. *et al.* Identification of the periplasmic cobalamin-binding protein BtuF of *Escherichia coli*. *J. Bacteriol.* **184**, 706–717 (2002).
15. Borths, E.L., Locher, K.P., Lee, A.T. & Rees, D.C. The structure of *Escherichia coli* BtuF and binding to its cognate ATP binding cassette transporter. *Proc. Natl. Acad. Sci. USA* **99**, 16642–16647 (2002).
16. Hvorup, R.N. *et al.* Asymmetry in the structure of the ABC transporter binding protein complex BtuCD-BtuF. *Science* **317**, 1387–1390 (2007).
17. Goetz, B.A., Perozo, E. & Locher, K.P. Distinct gate conformations of the ABC transporter BtuCD revealed by electron spin resonance spectroscopy and chemical cross-linking. *FEBS Lett.* **583**, 266–270 (2009).
18. Dassa, E. & Bouige, E. The ABC of ABCs: a phylogenetic and functional classification of ABC systems in living organisms. *Res. Microbiol.* **152**, 211–229 (2001).
19. Rees, D.C., Johnson, E. & Lewinson, O. ABC transporters: the power to change. *Nat. Rev. Mol. Cell Biol.* **10**, 218–227 (2009).
20. Borths, E.L., Poolman, B., Hvorup, R.N., Locher, K.P. & Rees, D.C. *In vitro* functional characterization of BtuCD-F, the *Escherichia coli* ABC transporters for vitamin B_{12} uptake. *Biochemistry* **44**, 16301–16309 (2005).
21. Chen, J., Sharma, S., Quiocho, F.A. & Davidson, A.L. Trapping the transition state of an ATP-binding cassette transporter: evidence for a concerted mechanism of maltose transport. *Proc. Natl. Acad. Sci. USA* **98**, 1525–1530 (2001).
22. Liu, C.E. & Ames, G.F. Characterization of transport through the periplasmic histidine permease using proteoliposomes reconstituted by dialysis. *J. Biol. Chem.* **272**, 859–866 (1997).
23. Merino, G., Boos, W., Shuman, H.A. & Bohl, E. The inhibition of maltose transport by the unliganded form of the maltose-binding protein of *Escherichia coli*: experimental findings and mathematical treatment. *J. Theor. Biol.* **177**, 171–179 (1995).
24. Ames, G.F., Liu, C.E., Joshi, A.K. & Nikaido, K. Liganded and unliganded receptors interact with equal affinity with the membrane complex of periplasmic permeases, a subfamily of traffic ATPases. *J. Biol. Chem.* **271**, 14264–14270 (1996).
25. van der Does, C., Presenti, C., Schulze, K., Dinkelaker, S. & Tampe, R. Kinetics of the ATP hydrolysis cycle of the nucleotide-binding domain of Mdl1 studied by a novel site-specific labeling technique. *J. Biol. Chem.* **281**, 5694–5701 (2006).
26. Pick, U. The interaction of vanadate ions with the Ca-ATPase from sarcoplasmic reticulum. *J. Biol. Chem.* **257**, 6111–6119 (1982).
27. Austermuhle, M.I., Hall, J.A., Klug, C.S. & Davidson, A.L. Maltose-binding protein is open in the catalytic transition state for ATP hydrolysis during maltose transport. *J. Biol. Chem.* **279**, 28243–28250 (2004).
28. James, K.J., Hancock, M.A., Gagnon, J.N. & Coulton, J.W. TonB interacts with BtuF, the *Escherichia coli* periplasmic binding protein for cyanocobalamin. *Biochemistry* **48**, 9212–9220 (2009).
29. Lundrigan, M.D., Koster, W. & Kadner, R.J. Transcribed sequences of the *Escherichia coli* btuB gene control its expression and regulation by vitamin B_{12}. *Proc. Natl. Acad. Sci. USA* **88**, 1479–1483 (1991).
30. Richter-Dahlfors, A.A., Ravnum, S. & Andersson, D.I. Vitamin B_{12} repression of the cob operon in *Salmonella typhimurium*: translational control of the cbiA gene. *Mol. Microbiol.* **13**, 541–553 (1994).
31. Van Hove, B., Staudenmaier, H. & Braun, V. Novel two-component transmembrane transcription control: regulation of iron dicitrate transport in *Escherichia coli* K-12. *J. Bacteriol.* **172**, 6749–6758 (1990).
32. Khare, D., Oldham, M.L., Orelle, C., Davidson, A.L. & Chen, J. Alternating access in maltose transporter mediated by rigid-body rotations. *Mol. Cell* **33**, 528–536 (2009).
33. Gorbulev, S., Abele, R. & Tampe, R. Allosteric crosstalk between peptide-binding, transport, and ATP hydrolysis of the ABC transporter TAP. *Proc. Natl. Acad. Sci. USA* **98**, 3732–3737 (2001).
34. Herget, M. *et al.* Purification and reconstitution of the antigen transport complex TAP: A prerequisite for determination of peptide stoichiometry and ATP hydrolysis. *J. Biol. Chem.* **284**, 33740–33749 (2009).
35. Chang, X.B., Hou, Y.X. & Riordan, J.R. ATPase activity of purified multidrug resistance-associated protein. *J. Biol. Chem.* **272**, 30962–30968 (1997).
36. Ozvegy, C., Varadi, A. & Sarkadi, B. Characterization of drug transport, ATP hydrolysis, and nucleotide trapping by the human ABCG2 multidrug transporter. Modulation of substrate specificity by a point mutation. *J. Biol. Chem.* **277**, 47980–47990 (2002).
37. Sauna, Z.E., Nandigama, K. & Ambudkar, S.V. Multidrug resistance protein 4 (ABCC4)-mediated ATP hydrolysis: effect of transport substrates and characterization of the post-hydrolysis transition state. *J. Biol. Chem.* **279**, 48855–48864 (2004).
38. Quiocho, F.A. & Ledvina, P.S. Atomic structure and specificity of bacterial periplasmic receptors for active transport and chemotaxis: variation of common themes. *Mol. Microbiol.* **20**, 17–25 (1996).
39. Eakanunkul, S. *et al.* Characterization of the periplasmic heme-binding protein shut from the heme uptake system of *Shigella dysenteriae*. *Biochemistry* **44**, 13179–13191 (2005).
40. Ho, W.W. *et al.* Holo- and apo-bound structures of bacterial periplasmic heme-binding proteins. *J. Biol. Chem.* **282**, 35796–35802 (2007).
41. Clarke, T.E., Braun, V., Winkelmann, G., Tari, L.W. & Vogel, H.J. X-ray crystallographic structures of the *Escherichia coli* periplasmic protein FhuD bound to hydroxamate-type siderophores and the antibiotic albomycin. *J. Biol. Chem.* **277**, 13966–13972 (2002).
42. Karpowich, N.K., Huang, H.H., Smith, P.C. & Hunt, J.F. Crystal structures of the BtuF periplasmic-binding protein for vitamin B_{12} suggest a functionally important reduction in protein mobility upon ligand binding. *J. Biol. Chem.* **278**, 8429–8434 (2003).

ONLINE METHODS

Protein purifications. We purified BtuCD, MetNI and Hi1470/1 as previously described[43–45]. We expressed BtuF and Hi1472 with a C-terminal Flag tag and purified them using anti-Flag M2 agarose (Sigma) from osmotic shock extracts. We expressed MetQ with an N-terminal decahistidine tag, and following purification, we removed the tag using enterokinase digestion according to the manufacturer's specifications (New England Biolabs). We concentrated protein samples to 5–10 mg ml^{-1} (Amicon Ultra concentrators, Millipore), snap froze them as small aliquots in liquid nitrogen and stored them at −80 °C for up to 3 months.

Reconstitution of BtuCD, MetNI and association experiments in liposomes. We reconstituted BtuCD essentially as previously described[20], except that we used 0.1% (w/v) *N*-dodecyl-*N*,*N*-dimethylamine *N*-oxide (LDAO) throughout the purification and reconstitution process. We reconstituted MetNI in a similar fashion, except that we used 0.05% (w/v) n-dodecyl-β-D-maltopyranoside (DDM) throughout. For association experiments with BtuF, we resuspended liposomes or proteoliposomes to a final concentration of 10 mg ml^{-1} lipids and 0.075 mg ml^{-1} protein in 50 mM Tris-HCl, pH 7.5, 150 mM NaCl. We then added Flag-tagged BtuF at the indicated concentrations (with additional additives where appropriate) and tilted the suspension at 25 °C for 10 min. We then spun the suspension for 20 min at 150,000*g*, removed the supernatant and resuspended the pellet with an equal volume of buffer + 1% (w/v) SDS. We visualized the amount of BtuF present in each fraction by immunoblot detection (using an anti-Flag antibody) after SDS-PAGE.

Size-exclusion chromatography. We injected 100- to 200-µl samples into a Superdex 200 10/300 column (GE Healthcare) mounted on an AKTA purifier system. We recorded absorbance at 280 nm or 360 nm as indicated. We removed excess vitamin B_{12} from BtuF by successive cycles, as indicated (**Fig. 4**), of tenfold dilution (with buffer devoid of vitamin B_{12}) and reconcentration using an Amicon Ultra concentrator (Millipore). Where applicable, we added 1 mM ATP, 50 µM EDTA, or 1 mM ATP, 2 mM $MgSO_4$, 1 mM orthovanadate, or 1 mM ADP, 2 mM $MgSO_4$, or 1 mM ATP, 2 mM $MgSO_4$, or 1 mM AMP-PCP, 2 mM $MgSO_4$, or 1 mM AMP-PNP, 2 mM $MgSO_4$ to both the column buffer and the injected sample.

Pulldown experiments. We immobilized purified, His-tagged BtuCD onto a Ni-NTA resin (10 microliters per sample), followed by a washing step to remove unbound protein. We added 250 µl of purified Flag-tagged MetQ at the indicated concentrations. Following a 10-min incubation, we removed unbound material by applying vacuum to Qiagen's miniprep spin-columns. We used six subsequent washes to insure complete removal of unbound protein. Where appropriate, we included nucleotides and/or substrate in the washing buffer. We then eluted bound material in a single step with buffer (100 µl) containing 1 M imidazole. We visualized the amount of retained Flag-tagged protein in the sample by standard immunoblot procedures, using an anti-Flag M2 HRP-conjugate antibody (Sigma).

BiaCore measurements. For ligand and analyte preparations, we took great care to remove all traces of aggregated material by using size-exclusion chromatography and ultracentrifugation (270,000*g*, 20 min). We immobilized BtuCD and Hi1470/1 onto a Ni-NTA chip, and MetNI to a CM-5 chip via an anti-pentahistidine antibody (Qiagen). We immobilized ~30 ng of the transporters per flow cell. We conducted all measurements at 25 °C, and the block compartment was cooled to 7–8 °C. We did not observe mass-transport limitations with BtuCD–BtuF or MetNI–MetQ, and we conducted experiments at a flow rate of 15 and 25 µl min^{-1}, respectively. Because of the slightly higher rates of the Hi1470/1 system, we used 50 µl min^{-1}. We ran experiments in 50 mM Tris-HCl, pH 7.5, 150 mM NaCl, 0.1% (w/v) *n*-dodecyl-*N*,*N*-dimethylamine *N*-oxide (LDAO) (BtuCD–BtuF), in 10 mM HEPES, 150 mM NaCl, 50 µM EDTA, 0.05% (w/v) *n*-dodecyl-β-D-maltopyranoside, pH 7.35 (MetNI–MetQ), or in 25 mM Tris-HCl, pH 7.5, 500 mM NaCl, 0.2% (w/v) *n*-decyl-β-D-maltopyranoside (Hi1470/1–Hi1472). Where appropriate, we added only substrates and/or nucleotides to the analyte's buffer. We collected data on BiaCore T100 or 2000 systems.

BiaCore data analysis and model fitting. All models used for fitting of the experimental data are part of the Biacore evaluation software. Despite the clear biphasic nature of the association curves, we initially attempted fitting by applying a simple one-to-one binding model. As expected, the statistics and fit quality of these preliminary fits were poor. Then, for each of the experiments shown, we applied a model that accounts for a possible conformational change following complex formation $A+B \leftrightarrow AB \leftrightarrow AB$, where A and B represent the transporter and binding protein. In this model, k_{a1} and k_{d1} are the forward and reverse rate constants for complex formation, and k_{a2} and k_{d2} are the forward and reverse rate constants for the conformational change. The overall dissociation constant for this scheme, K_d, is related to the rate constants through the expression:

$$K_d = \frac{[A][B]}{[AB]+[AB']} = \frac{k_{d1}k_{d2}}{k_{a1}(k_{d2}+k_{a2})} \quad (1)$$

A more detailed description of the parameters and equations is provided in the BiaCore (GE Healthcare) T100 Software Handbook (BR-1006-48, edn. AE, 186–187).

43. Locher, K.P., Lee, A.T. & Rees, D.C. The *E. coli* BtuCD structure: a framework for ABC transporter architecture and mechanism. *Science* **296**, 1091–1098 (2002).
44. Pinkett, H.W., Lee, A.T., Lum, P., Locher, K.P. & Rees, D.C. An inward-facing conformation of a putative metal-chelate type ABC transporter. *Science* **315**, 373–377 (2007).
45. Kadaba, N.S., Kaiser, J.T., Johnson, E., Lee, A. & Rees, D.C. The high-affinity *E. coli* methionine ABC transporter: structure and allosteric regulation. *Science* **321**, 250–253 (2008).

doi:10.1038/nsmb.1770